МАТЕРИАЛОВЕДЕНИЕ В МАШИНОСТРОЕНИИ

UDC 621.78:669.14

SHIPITSYN Sergey Ya., D. Sc. in Eng.
Head of the Laboratory[1]
E-mail: odus@kiev.ptima.ua

ZHORNIK Viktor I., D. Sc. in Eng., Assoc. Prof.
Head of the Department of Technologies of Mechanical Engineering and Metallurgy — Head of the Laboratory of Nanostructured and Superhard Materials[2]
E-mail: zhornik@inmash.bas-net.by

ISAEVA Lyudmila E., Ph. D. in Chem.
Associate Professor of the Department of Theory of Metallurgical Processes and Chemistry[3]
E-mail: isaevanmetau@gmail.com

KUCHERENKO Pavel N.
Junior Researcher[1]
E-mail: odus@kiev.ptima.ua

LIHOVEY Dmitry I.
Junior Researcher[1]
E-mail: odus@kiev.ptima.ua

[1]Physico-Technological Institute of Metals and Alloys of the NAS of Ukraine, Kiev, Ukraine
[2]Joint Institute of Mechanical Engineering of the NAS of Belarus, Minsk, Republic of Belarus
[3]National Metallurgical Academy of Ukraine, Dnipro, Ukraine

Received 23 July 2019.

METAL SCIENCE ASPECTS OF THE INFLUENCE OF DISPERSION NITRIDE HARDENING ON THE STRUCTURE OF HYPOEUTECTOID AND EUTECTOID CARBON STEELS

The article presents the results of metal science research on the influence of nitrogen and vanadium microalloying of carbon steels with a carbon content of 0.5–0.8 wt.% on the thermodynamic and thermokinetic parameters of the phase redistribution of nitrogen and vanadium, as well as the formation of ferrite-pearlite, bainite and martensite structures and their transformation during high tempering. It was shown that the dispersion of the structure formed during cooling after austenitization, as well as the decrease of the growth rate and coagulation of cementite particles are the result of dispersion of the pearlite, bainite and martensite tempering structures. The positive effect of the dispersion of structures of all levels on the improvement of the mechanical properties (yield point, impact toughness, wear resistance under sliding and rolling friction, etc.) of the steel modified by nitrogen and vanadium microalloying is noted. That provides good prospects for the effective use of steels with dispersion nitride hardening for the production of railway wheels and rails.

Keywords: *carbon steels, alloying, dispersion nitride hardening, ferrite-pearlite, bainite and martensite structures, austenitization, tempering, phase transformations, railway wheels and rails*

Introduction. Medium- and high-carbon hypoeutectoid and eutectoid steels of high strength and wear resistance are widely used in various branches of mechanical engineering [1]. However, they are most widely used for production of railway wheels and rails. Technical and economic indicators of railway vehicles are

the main way to determine reliability and operational life of railway wheels and rails, which are in extremely harsh operating conditions. At the same time, the existing wheel and rail steels no longer meet modern requirements for higher speeds and rolling stock carrying load. This refers both to Ukraine and to countries of near and far abroad. The main reason for this is the use of relatively cheap unalloyed and low-alloyed medium and high carbon pearlite class steels for production of rails and wheels. In particular, according to GOST 10791-2011 (Russian Federation) and the international standard ISO 1005-1994 of railway wheels are produced with the steel with chemical composition, wt.%: 0.44–0.77 C; 0.50–1.25 Mn; 0.22–0.65 Si; 0.05–0.15 V; 0.005–0.040 S; ≤ 0.030–0.040 P. According to the European standard prEN 13674-1, GOST 4344-2004 and GOST R 51685-2013 (Russian Federation) railway rails are made of steel, wt.%: 0.38–0.82 C; 0.65–1.75 Mn, 0.13–1.12 Si; 0.00–0.20 V; 0.00–1.25 Cr; 0.00–0.01 N; 0.008–0.045 S; ≤ 0.04 P.

In steels of these classes increase of static strength due to increase of carbon content is accompanied by decrease of cyclic strength, static and cyclic fracture toughness, ductility, contact endurance [2, 3]. Moreover, they have insufficient thermal fatigue strength, heat and cold resistance, and are prone to the formation of austenitic layers with subsequent $\gamma \rightarrow M$ transformation when the surface zones are locally heated to temperatures above Ac_1 и Ac_3 during skidding and slipping of the wheel.

Systemic fundamental researches at Physico-Technological Institute of Metals and Alloys of the NAS of Ukraine within several decades and accumulated experience in industrial application have shown that dispersion nitride-vanadium hardening technology provides a significant increase in the whole range of physico-mechanical and operational properties of cast and deformed carbon, low-alloyed and alloyed steels of various functional purposes. It was found for the first time that a necessary condition for the effective implementation of microalloying with nitrogen and vanadium is not only optimization of the dispersion nitride hardening process, but also taking into account the effect of nitrogen on crystallization processes and the development of primary chemical and structural heterogeneity of the metal, austenite grain size, and pearlitic thermodynamic parameters, bainitic and martensitic transformations, morphology of carbide phases during the decomposition of a supersaturated austenite and ferrite solid solution, the development of secondary chemical and structural heterogeneity, including grain boundary.

The most significant advantage of the steels developed at Physico-Technological Institute of Metals and Alloys of the NAS of Ukraine is a simultaneous significant increase in their static and cyclic strength, static and cyclic fracture toughness, thermal resistance, wear resistance, hardenability, weldability, reduction or complete elimination of the tendency to natural, deformation and thermal embrittlement [4].

This paper presents the results of experimental researches that show a high efficiency of dispersion nitride hardening technology use for significant improvement of the physical, mechanical and functional properties of hypoeutectoid and eutectoid steels used in the manufacturing of railroad wheels and rails.

Methods and techniques of experiments. *Smelting of prototype steels.* Steels were smelted in induction furnaces IST-0.16 with a crucible capacity of 30 kg and BIN-3 with a crucible capacity of 3.5 kg. The crucible lining is acid. Melting under the composition flux (wt.%): lime CaO – 50 + quartz sand SiO_2 – 30 + fluorspar CaF_2 – 20. Steels were poured into dry sand-clay or cast-iron molds. As a charge for steelmaking the following were used: unalloyed low-carbon steel scrap of brand 10864 GOST 11036-75; silicon of technical brand Kr00 GOST 2169-69; metal manganese Mr00 GOST 6808-90; ferrovanadium with 43 % V GOST 27130-94; synthetic cast iron with 4.59 wt.% carbon; aluminum AV97 DSTU 3753-98; nitrated ferrochrome of brands FKhN 100A and FKhN 100B GOST 4757-91, silicocalcium of brand SK30 GOST 4762-71. After antiflake annealing, cast ingots were rolled at 900–1100 °C and a degree of deformation of 40–50 % onto sample blanks of the required shape and size. The chemical composition of the steels was determined on cast samples. The concentration of carbon, sulfur, phosphorus was determined by chemical analysis according to DSTU 123-44-2005, DSTU 12347-77, DSTU 123-45-2004. The nitrogen concentration was determined by reduction smelting method by smelting the sample in helium flow with purity of 99.99 % using the "LECO" analyzer with the accuracy of 10^{-4} wt.%. The concentration of other elements was determined by spectral analysis according to GOST 8895-97.

Chemical phase analysis of nitrogen and vanadium distribution between VN, [V], [N]. The effect of the carbon concentration on the thermodynamic parameters of nitrogen and vanadium redistribution between VN nitride and solid solution [V] and [N] was studied on steels that contain carbon in the range of 0.50–0.80 wt. % (Tables 1, 2).

Separation of VN nitride phase from steels was carried out by the method of anodic electrochemical dissolution of the metal base of samples followed by chemical analysis of the separated precipitates [5]. The electrolysis was carried out in an aqueous electrolyte of the composition (wt.%): 15NaCl + $2.5C_4H_6O_6$ in the potentiostatic mode, which was provided by the electronic block potentiostat "10-20 PEB". A part of the nitride precipitate was subjected to X-ray diffraction analysis using a DRON-2 refractometer in copper monochromatized radiation with interpretation of the X-ray diffraction patterns using an ASTM data file to confirm the presence of VN nitrides close to stoichiometric in the precipitate. Another part of the precipitate was used to determine its composition by the chemical method. The nitrogen concentration was determined by steam aspiration [5] by the color intensity on KFK-2PM

Table 1 — Chemical composition (wt.%) of the steels under study

Steel brand	C	Si	Mn	Cr	Ni	Mo	Al	Cu	Co	V	Ca	Ce	Zr	La	N	Se
50SGAF	0.50	0.58	1.25	0.39	0.091	0.015	0.014	0.029	0.007	0.220	0.0012	<0.002	0.0028	0.0006	0.020	<0.002
60SGAF	0.59	0.46	1.20	0.42	0.094	0.012	0.009	0.022	0.011	0.195	0.0013	<0.002	0.0027	0.0003	0.021	<0.002
60SGF	0.60	0.45	1.19	0.10	0.085	0.011	0.015	0.019	0.090	0.205	0.0011	<0.002	0.0013	0.0003	0.004	<0.002
80SGAF	0.80	0.51	1.31	0.29	0.087	0.014	0.013	0.026	0.010	0.210	0.0012	<0.002	0.0015	0.0016	0.019	<0.002
Note: 1) the analysis was carried out on the "Spectromax" equipment (Germany); 2) content in steels (wt.%): S – 0.015...0.018; P – 0.0017...0.0250																

Table 2 — Chemical composition of prototype steels (wt.%)

Steel brand	C	Si	Mn	V	N	Cr	S	P	Al
70GF	0.68	0.35	1.1	0.09	0.004	—	0.021–0.024	0.015–0.019	0.015–0.021
70GAF	0.69	0.37	1.2	0.11	0.013	0.029	0.021–0.024	0.015–0.019	0.015–0.021
80G2SF	0.85	0.45	1.70	0.13	0.0037	0.40	0.024	0.055	—
80G2SAF	0.79	0.43	1.64	0.17	0.0100	0.69	0.017	0.049	—

photocolorimeter. The vanadium content in the precipitate was determined by the redox method based on the dissolution of the of the nitride precipitate in acids, oxidation of vanadium ion (VO^{2+}) with potassium permanganate, and titration of the solution with phenylanthranilic acid [6]. The determination accuracy of V and N concentration in the precipitate was ±0.001 % for vanadium, ±0.0001 % for nitrogen.

Dilatometric research on the effect of dispersion nitride hardening on the thermokinetic transformations parameters $\gamma \rightarrow \alpha$ (pearlite, bainite, martensite). The research was carried out on prototype steels with (80G2SAF) and without dispersion nitride hardening (80G2SF) using quartz dilatometer of the design of G.V. Kurdyumov Institute for Metal Physics of the NAS of Ukraine. Samples with dimensions d = 4 mm and l = 20 mm were placed in a sealed chamber of the dilatometer; air was pumped out to the pressure of 10^{-1} MPa. After that the chamber was filled with an inert gas, helium. The samples were heated to austenitization temperature (860 °C for steel 80G2SF; 1000 °C for steel with dispersion nitride hardening 80G2SAF). The heating was carried out with a maximum heating rate of 1.2 °C/s. Isothermal soaking at austenitization temperature takes 10 min. All samples were cooled to temperature above Ar_3 (800 °C) in a helium atmosphere and in cases when the temperature is lower the cooling was carried out in the air with additional cooling (cooling fan) and without it in the range of initial cooling rate 3.5–10 °C/s. It was necessary to fix the time-temperature parameters $\gamma \rightarrow \alpha$ of transformation in the zones of diffusion (pearlite), intermediate (bainite) and shear (martensite) transformations.

X-ray diffraction analysis and research on the tempering temperature effect on the hardness of steels with different structures after austenitization (pearlite, bainite, martensite). The research was carried out on 70GF and 70GAF steels with and without dispersion nitride hardening. X-ray diffraction analysis was performed on a DRON-3 diffractometer equipped with the "Diffwin" automated software package. Taking of the X-ray diffraction photograph was carried out in monochromatic SoKα radiation.

The results of the research and their discussion. *Thermodynamic parameters of nitrogen and vanadium phase distribution during austenitizing heating and tempering.* Optimal results for improving the physico-mechanical and functional properties of steels by dispersion nitride hardening technology are achieved by dispersion and stabilization of austenitic grain during austenitizing heating and effective dispersion hardening of the ferrite matrix with nitride nanoparticles of VN at high temperature tempering. In the works [4, 7], it was established that this condition could be achieved in case of 10–15 % of the primary nitride phase during austenitizing heating. This phase blocks the growth of the austenitic grain. It was also found that there is a need for dispersion precipitation of the nitride phase during high-temperature tempering not less than 40–50 % of the theoretically possible amount of this phase with a complete binding of nitrogen and vanadium in steel to the VN nitrides of stoichiometric composition.

In order to determine the optimal temperature and time parameters of austenitizing heating and high-temperature tempering of high-carbon steels with dispersion nitride hardening, we studied the effect of the carbon contained in them on these parameters.

By chemical and X-ray diffraction analysis in steels with different carbon concentration of 0.50–0.80 wt.% and the same concentration of impurity elements (see Table 1), the phase distribution of nitrogen and vanadium was studied at austenitizing heating temperatures in the range of 850–1000 °C and tempering in the range of 450–600 °C. The duration of the austenitizing heating was 2 hours and the high-temperature tempering was 4 hours. According to the data of works [4, 7, 8], such an austenitizing heating duration provides the achievement of phase equilibrium conditions in VN-[V]-[N] system of structural carbon steels, and the duration of high-temperature tempering is close to the actual conditions of industrial production of high-carbon steel products [8].

The experimental data are shown in the tables (Tables 3 and 4).

Table 3 — Content of vanadium, nitrogen and vanadium nitrides in the electrolytic precipitation of high carbon steels after austenitization

Brand	VN_{max}	$T_{aust.}$, °C	wt.% in precipitation after austenitization				$VN_{aust.}$
			V	N	VN	V/N	
50SGAF	0.0928	850	0.053	0.0116	0.538	4.57	58
		900	0.035	0.0087	0.0404	4.02	43.5
		950	0.011	0.0028	0.0130	3.93	14
		1000	0	<0.0001	0	0	0
60SGAF	0.0974	850	0.028	0.0072	0.0334	3.89	34.3
		900	0.019	0.003	0.0139	6.3	14.3
		950	0	<0.0001	0	0	0
		1000	0	<0.0001	0	0	0
60SGF	—	850	0.005	0	0	0	0
		900	0	0	0	0	0
		950	0	0	0	0	0
		1000	0	0	0	0	0
80SGAF	0.0882	850	0.007	0.0013	0.0177	5.5	20.1
		900	0.006	0.0009	0.0042	6.22	4.8
		950	0	<0.0001	0	0	0
		1000	0	<0.0001	0	0	0

Note: 1) VN_{max} — the maximum theoretically possible amount of VN in steel; 2) $VN_{aust.}$ — the amount of VN after austenitization in percentage of the maximum theoretically possible amount of VN in steel

Table 4 — Content of vanadium, nitrogen and vanadium nitrides in the electrolytic precipitation of high carbon steels after austenitization and tempering

Steel brand	VN_{max}, wt.%	$T_{aust.}$, °C	Content in precipitation after austenitization				Content in precipitation after tempering				
			V	N	VN	$VN_{aust.}$, %	$T_{temp.}$, °C	V	N	VN	$VN_{temp.}$, %
			wt.%					wt.%			
50SGAF (0.22%V; 0.020%N)	0.0928	940	0.012	0.0030	0.0139	15.0	450	0.011	0.0028	0.0127	13.7
							500	0.013	0.0028	0.0129	13.9
							550	0.019	0.0039	0.0275	29.6
							600	0.034	0.0088	0.0408	44.0
60SGAF (0.195%V; 0.0210%N)	0.0974	910	0.017	0.0029	0.0135	13.7	450	0.016	0.0028	0.0133	13.7
							500	0.015	0.0032	0.0139	14.3
							550	0.025	0.0101	0.0227	23.3
							600	0.036	0.0091	0.0423	43.4
80SGAF (0.210%V; 0.019%N)	0.0882	900	0.006	0.0009	0.0042	4.7	450	0.007	0.0013	0.0061	6.9
							500	0.006	0.0012	0.0068	7.7
							550	0.008	0.0041	0.0204	23.1
							600	0.031	0.0085	0.0395	44.8

Note: 1) VN_{max} is the maximum theoretically possible amount of VN in steel; 2) $VN_{aust.}$ is the amount of VN in the precipitate after austenitization as a percentage of the maximum theoretical amount of VN in steel (VN_{max}); 3) $VN_{temp.}$ is the amount of VN in the precipitate after tempering as a percentage of the maximum theoretical amount of VN in steel (VN_{max})

The reliability of the data in Table 3 is confirmed by the analysis of austenitic grain growth in 60CGAF steel when the austenitizing heating temperature increases. Thus, at heating temperatures of 850 and 900 °C the austenite grain grade (GOST 5639-82) is 9.0–9.5, and at temperatures of 950–1000 °C when the nitride phase dissolves, it decreases to 6.0–7.0. The average size of austenitic grain (d_{avg}) in the first case is 10–15 μm. At the same time in the steel 60GSF without dispersion nitride hardening, the austenitic grain grade score decreases from 7 (d_{avg} = 35 μm) to 4.5–5.0 (d_{avg} = 60–80 μm) when the temperature of austenitizing heating increases from 850 to 1000 °C.

This means that the nitrogen and vanadium alloying of high-carbon steels with the purpose of their additional effective dispersion nitride hardening provides a reduction of 2.5–3.0 times the size of the austenitic grain at austenitization in the temperature range of 850–1000 °C due to the excess high-temperature dispersion nitride-vanadium phase that does not dissolve during austenitization.

The amount of solid solution nitrogen and vanadium in the steels during austenitizing heating was determined by the difference in the content of elements in steel and precipitation. Taking into account that in the logarithm equation of the product of equilibrium quantities of solid solutions of nitrogen and vanadium $\lg[V][N] = A/T + B$ (T is the temperature, A, B are the coefficients), the dependence of $\lg[V][N]$ on $1/T$ is linear (Figure 1), the coefficients A and B were determined by the least squares method according to the formulas:

$$y = A_1 x + A_0; \quad (1)$$

$$A_1 = (\Sigma x \cdot y - \Sigma x \cdot \Sigma y) / n / (\Sigma x^2 - (\Sigma x)^2)/n; \quad (2)$$

$$A_0 = (\Sigma y - \Sigma x \cdot A_1) / n; \quad (3)$$

$$\varepsilon = (\Sigma y^2_{exp} - \Sigma y^2_{calc}) / \Sigma y^2_{exp}, \quad (4)$$

where x — $1/T$, K; y — lg[V][N]; A_1, A_0 — are the coefficients A and B in the formula (1); ε — the experimental error, %.

The calculated empirical formulas lg[V][N] in the steels with different carbon content are as follows:

- for the steel 50SGAF:

$$\lg[V][N] = -5840/T + 2.3; \quad (5)$$

- for the steel 60SGAF:

$$\lg[V][N] = -4290/T + 1.18; \quad (6)$$

- for the steel 80SGAF:

$$\lg[V][N] = -4286/T + 1.39 \quad (7)$$

when the experimental error is 0.012–0.020 %.

The calculation using formulas (1)–(3) showed that the equilibrium temperature of complete dissolution of VN particles with a composition close to the stoichiometric (see Table 3) decreases with increasing carbon content in the steel: 50SGAF — 981 °C, 60SGAF — 942 °C, 80SGAF — 898 °C.

Processing of these data using the least squares method made it possible to establish the dependence of the decrease in the equilibrium dissolution temperature of vanadium nitrides in austenite (t_{VN}) on the carbon content in the steel in the form:

$$t_{VN} = 980 - 33.3 \cdot n, \text{ °C}, \quad (8)$$

where 980 — the t_{VN} temperature with 0.5 wt.% carbon, °C; coefficient 33.3 indicates a decrease in t_{VN} temperature with an increase in carbon content by 0.1 wt.%, °C; n is the amount of 0.1 wt.% carbon in the steel in the range of 0.5–0.8 wt.%, counting from 0.5.

An increase in the carbon content in steel, both in austenite and in ferrite, reduces the activity of nitrogen to vanadium. In the case of dissolution of vanadium nitrides in austenite, this leads to a decrease in the equilibrium temperature of their dissolution. According to thermodynamic parameters, the same effect should be observed for homogeneous release of vanadium nitrides at high tempering, i. e. the temperature of the effective dispersion precipitation VN should decrease.

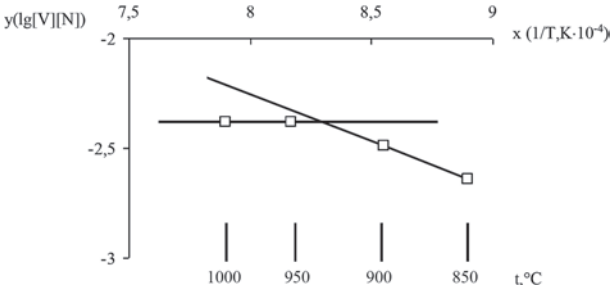

Figure 1 — Graphical dependence of lg[V][N] on $1/T$ for 60SGAF wheel steel according to chemical phase analysis data

However, experimental data (Figure 2) show that an increase in the carbon content in the steel practically does not affect the temperature of the effective dispersion precipitation of vanadium nitrides, i. e. the tempering temperature at which about 50 wt.% of nitrides are dispersed from the theoretical amount in the case of complete binding of nitrogen and vanadium in the steel in the nitride phase.

At the same time, with an increase in the tempering temperature due to an increase in the diffusion mobility of the elements the amount of the dispersion nitride phase naturally increases. Its necessary amount (about 50 % of the theoretically possible) can be reached at temperatures of about 600 °C. This is due to the fact that during the tempering of the steel, the thermokinetic factor, rather than the thermodynamic one, predominantly influence on the process of dispersive separation of the nitride-vanadium phase.

Structure formation during cooling after austenitizing heating. The purpose of the research on the effect of the cooling rate after austenitization on the temperature-time dependences of phase transformations is to determine the technological parameters of hardening of railway rails and wheels made of steel with dispersion nitride hardening, which will ensure the formation of an optimal metal structure. In order to achieve maximum wear resistance of the rolling surface of rails and wheels, thin-plate pearlite with bainite admixtures is used as such structure. According to the works [2, 3, 7, 8], such structure can be formed in standard rail and wheel steels at initial cooling rates in the range of 5–10 °C/s after austenitizing heating.

Researches using dilatometric analysis method were carried out on hot-deformed steels close in chemical composition to standard rail steels without dispersion nitride hardening (steel 80G2SF) and with dispersion nitride hardening (steel 80G2SAF) (see Table 2).

Studies have shown that dispersion nitride hardening significantly affects the temperature-time parameters of phase transformations and structural parameters

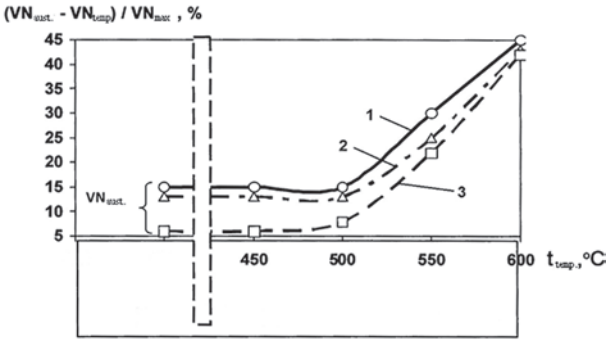

Figure 2 — The amount of nitride-vanadium phase in the steel precipitation after austenitization at the optimal temperature ($VN_{aust.}$) and tempering ($VN_{temp.}$) as a percentage of the maximum theoretical amount of VN in steel: 1 — Steel 50SGAF (0.22 % V; 0.020 % N); $t_{aust.}$ = 940 °C; 2 — 60SGAF (0.195 % V; 0.0210 % N); $t_{aust.}$ = 910 °C; 3 — 80SGAF (0.210 % V; 0.019 % N); $t_{aust.}$ = 900 °C

of high-carbon steel depending on the cooling rate after austenitization. Figure 3 shows data indicating a decrease in the temperature ranges of pearlite, bainite and martensitic transformations in the steel during cooling after austenitization. This is due to increase in the stability of austenite with solid-solution nitrogen, both upon cooling and upon heating of the metal [4].

The data shown in Figure 4 reflect the effect of the cooling rate on the phase composition of steels. These data show that dispersion nitride hardening affects not only the reduction of temperature intervals $\gamma \rightarrow \alpha$ (pearlite, bainite, martensite) transformations, but also the phase composition of the metal structure at close sample cooling rates. The austenitizing heating temperature of steel 80G2SF is 860 °C. It corresponds to the standard for rail steels. Meanwhile the austenitizing heating temperature of steel 80G2SAF is 920 °C, which provides the necessary phase distribution of nitrogen and vanadium during austenitization.

It is shown that formation of bainite and martensite structures in steels with dispersion nitride hardening occurs at the initial cooling rate, which is 15 % less than the cooling rate of standard steel. In particular, the formation of bainite and martensite structures in standard steel occurs at an initial cooling rate of 10 °C/s, and in steel with dispersion nitride hardening it is 8.5 °C/s. The dispersion of the structural components of pearlite, bainite and martensite structures of steel increases (Figure 5).

Structure formation during high temperature tempering. Figure 6 shows the structures after tempering standard steel and nitride-hardened steel, which were preliminarily normalized to plate pearlite, hardened to martensite and subjected to isothermal hardening to bainite. It can be seen that despite the difference in tempering temperature (450 °C for the standard steel and 600 °C for the steel with dispersion nitride hardening), in the steel with dispersion nitride hardening the tempering structures of pearlite, bainite and martensite are similar or even more dispersed than those of standard steel. This is mainly due to the dispersion of

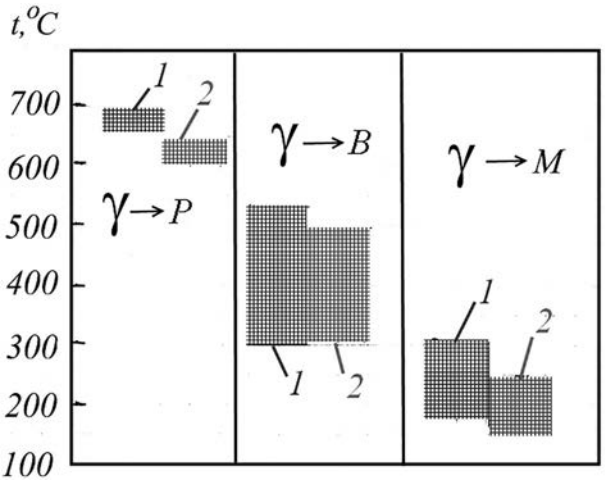

Figure 3 — Temperature ranges of $\gamma \rightarrow P$, $\gamma \rightarrow B$, $\gamma \rightarrow M$ transformations when cooling 80G2SF (1) and 80G2SAF (2) steels

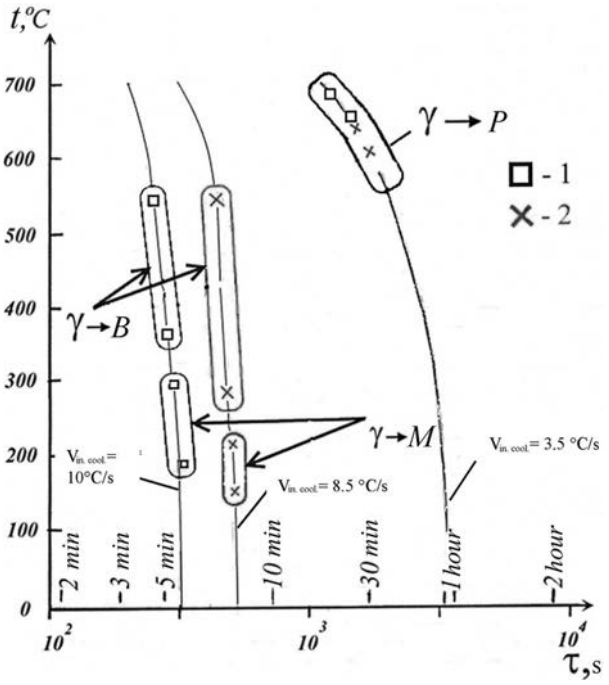

Figure 4 — Fragments of thermokinetic decomposition diagrams of supercooled austenite of the steels: 1 — □ — steel 80G2SF, $t_{aust.}$ = 860 °C; 2 — × — steel 80G2SAF, $t_{aust.}$ = 920 °C, $V_{in.cool.}$ is the initial cooling rate of samples from the austenitization temperature

previous structures of pearlite, bainite and martensite and changes in the conditions of nucleation, growth and coagulation of the cementite phase.

It is known that at low tempering (150–300 °C) of hardened steels under conditions of low diffusion mobility of carbon and iron atoms and alloying elements, nucleation of centers and partial separation of disperse (about 10^{-6} cm) coherent plate form of cementite carbides (ε-carbide) occurs in places of carbon segregation. Those places are most likely to be dislocations in martensite crystals and microtwins [9, 10]. The alloying elements have almost no effect on the precipitation of the carbide phase at low tempering [11].

At high tempering (≥ 450 °C) of hardened steels the mechanism of influence of alloying with nitrogen and vanadium on the formation of micro- and fine structures is more complex. It can additionally consist of the following effects: nitrogen segregations which did not dissolve during austenitization and parts of nitride phase that was released during tempering on the mobility of dislocations, polygonization and recrystallization processes; vanadium on the activity and diffusion mobility of carbon, and nitrogen on the activity of vanadium to carbon; incoherent particles of the nitride phase on the diffusion direction of vacancies, atoms of the elements of introduction and substitution, the centers of special carbides emergence.

The last thesis statement is analyzed in detail in the work [12]. Its essence is as follows. It is known amongst places of vacancy runoff, interstitial, substitutional and precipitation impurities of the secondary phases are interphase boundaries of matrix-inclusion interface and stress state zones formed under its influ-

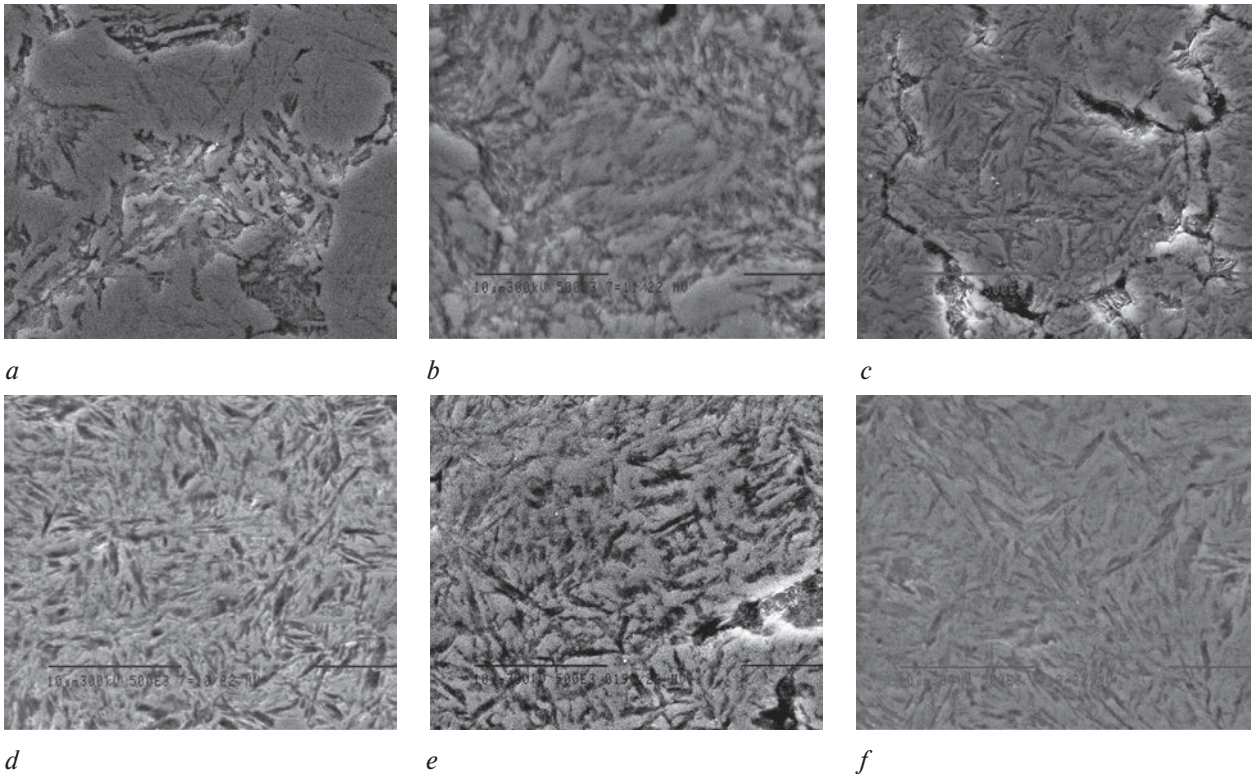

Figure 5 — Microstructures of the steels 80G2SF (*a*, *c*, *e*) and 80G2SAF (*b*, *d*, *f*) (×5000): *a*, *b* — ferrite-pearlite structure (initial cooling rate $V_{in.cool.}$ is 3.5 °C/s); *c*, *d* — bainite structure ($V_{in.cool.}$ is 10 °C/s for steel 80G2SF, 8.5 °C/s for steel 80G2SAF); *e*, *f* — martensite-bainite structure ($V_{in.cool.}$ is 10 °C/s for 80G2SF, 8.5 °C/s for 80G2SAF)

ence [13–20], including compression and extension components near angular inclusions [21]. According to the data of the works [22, 23], the segregation capacity of high-angle intergranular and interphase boundaries is much larger than that of low-angle ones.

Researches by the article authors and other specialists of the School of Corresponding members of the National Academy of Sciences of Ukraine named after Yu.Z. Babaskin showed that in perlitic and martensitic steels, as well as in single-phase ferritic and austenitic steels of different classes under the optimal mode of dispersion nitride hardening, the number of statistically uniformly, intragrainally separated VN particles is no more than 0.02–0.04 wt.%. With their size of about

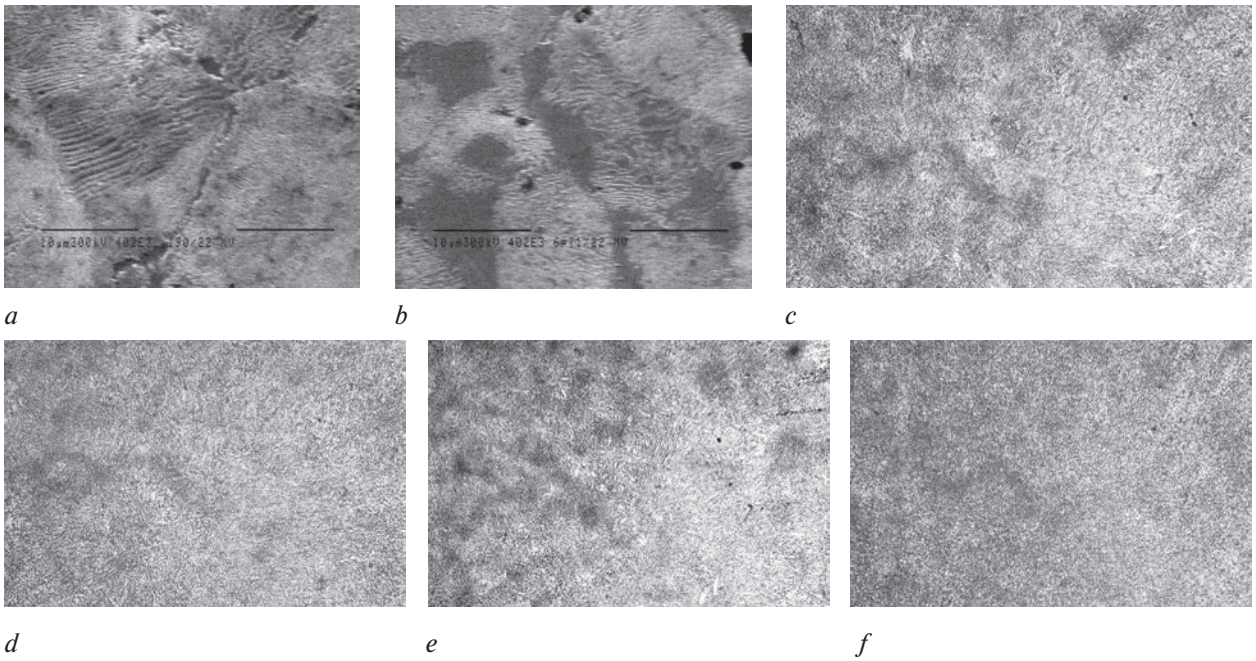

Figure 6 — Structures of the standard steel 80G2SF (*a*, *c*, *e*) and the steel with dispersion nitride hardening 80G2SAF (*b*, *d*, *f*) with initial ferrite-pearlite (*a*, *b*) (×5000), bainite (*c*, *d*) (×1000) and martensite (*d*, *e*) (×1000) structure after tempering at 450 °C (steel 80G2SF) and 600 °C (steel 80G2SAF)

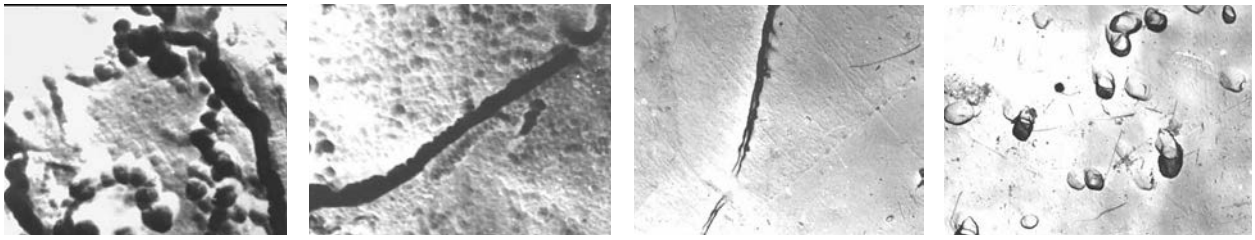

a *b* *c* *d*

Figure 7 — Carbide phase distribution of cast steels 25Kh3GL (*a*) and 25Kh3GAFL (*b*) in intergranular boundary areas after normalization (×41 000) and hot-rolled single-phase ferrite steels 04Kh18T (*c*) and 04Kh18AF (*d*) (×4000) without polymorphic transformations. Steels 25Kh3GL and 04Kh18T without VN phase, 25Kh3GAFL and 04Kh18AF with VN phase [4]

30–40 nm and an interparticle distance of 200–500 nm, the total area of the VN-matrix interfacial boundaries and the volumes of the distorted crystal lattice near them are 2–3 orders of magnitude higher than these indicators for high-angle intergrain boundaries, as well as interphase boundaries of the "massive cementite and special carbide particles". Energy-efficient areas for diffusion of interstitial elements (carbon) inside of them and formation of carbide phases (they are called diffusion-energy "traps") change the direction of diffusion flows from high-angle intergranular and interphase boundaries "massive carbide inclusions-matrix" to diffusion-energy "traps".

This provides almost complete suppression of grain boundary segregation of carbon and carbide phases and decreases the growth and coagulation rate of carbide phases at high-temperature tempering (Figure 7).

In the case of steels with pearlite and bainite structures in which carbides of cementite type are fully or partially formed, the effect of nitrogen and vanadium alloying is already related to changes in the intensity and direction of diffusion of carbon and iron which is responsible for the process of growth and coagulation of carbide phases.

An integral indicator of the effect of nitrogen and vanadium alloying on the formation of micro- and fine structure, as well as distortion of the crystal lattice during tempering is the hardness of steel. Figure 8 shows data on the dependence of the steel hardness on the tempering temperature. From the data presented, it can be concluded that for all types of initial structure (pearlite, bainite, martensite) alloying steel with nitrogen and vanadium naturally increases its hardness throughout the temperature range of tempering.

This is a result of dispersion of the main hardening phase that is presented by carbides of cementite type and additional dispersion hardening of ferrite by vanadium nitride particles. In the case of increasing the austenitizing heating temperature of the steel 70GF to 970 °C as for the steel 70GAF, the difference in hardness of the steels would be even greater due to a hardness decrease of the first one due to an intensive growth of austenitic grain, a transformation temperature $\gamma \rightarrow \alpha$ (pearlite, bainite, martensite) increase and coarsening of the tempering structures of pearlite, bainite, martensite.

X-ray diffraction researches of the fine structure of tempered steels have shown that alloying with nitrogen and vanadium causes, firstly, a certain (1.5–2 times) reduction in the size of coherent blocks of the ferrite crystal lattice of different orientations both at the initial martensite and pearlite structure; secondly, a significant (4 times) decrease in microdistortions of the ferrite lattice; thirdly, a significant (almost 30 times) decrease in

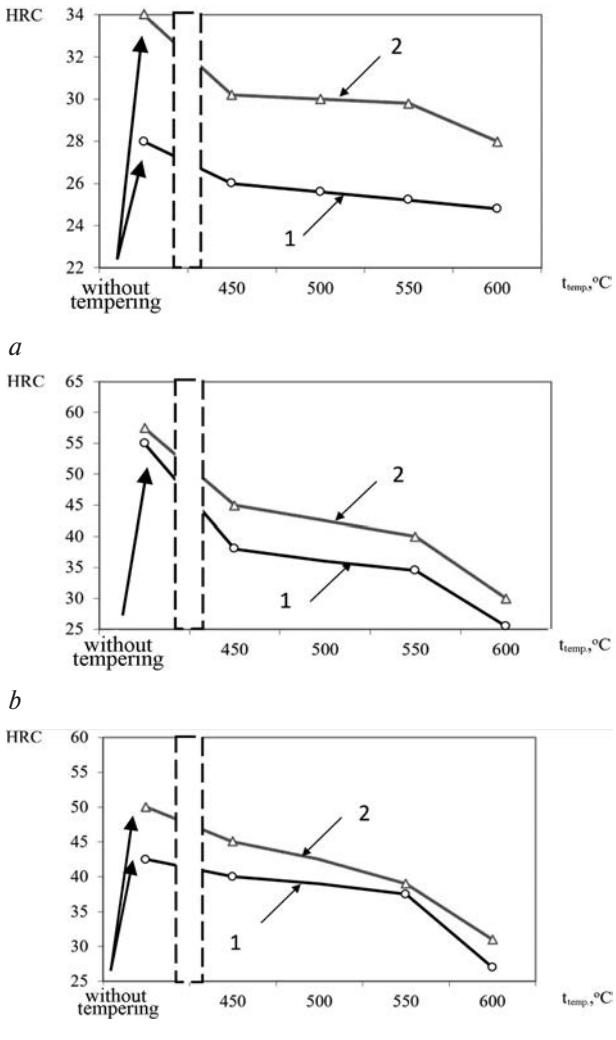

Figure 8 — Effect of tempering temperature on the hardness of the standard steel 70GF (1) and the steel with nitride hardening 70GAF (2), normalized to pearlite (*a*), hardened to martensite (*b*) and after isothermal hardening to bainite (*c*). Austenitization temperatures: 850 °C for 70GF; 970 °C for 70GAF

Table 5 — Parameters of the fine crystal structure of tempered ferrite steels

Parameters	Steel brand			
	70GF		70GAF	
	Initial structure after austenitization			
	martensite	pearlite	martensite	pearlite
Crystal lattice parameters of the matrix a, nm	0.2868	0.2864	0.2862	0.2868
Average size of coherent scattering of X-ray zones D, nm	1.10	1.57	0.65	1.02
Microdistortions of the crystal lattice $\Delta a/a \cdot 10^2$	0.36	0.45	0.09	0.50
Root-mean-square deviation of atoms from the equilibrium position $\sqrt{\overline{u}^2}$	0.41	0.35	0.33	0.35
Dislocation density ρ, 10^{-16}, м$^{-2}$	0.560	0.382	0.020	0.781
Note: tempering temperature of steels: 450 °C for 70GF, 600 °C for 70GAF; temperature of austenitizing heating of steels: 860 °C for 70GF; 970 °C for 70GAF				

the density of dislocations in ferrite with an initial martensitic structure (Table 5). These factors are predicted by an increase in the ductility and viscosity of the metal while maintaining its strength.

This estimation was confirmed by data on the properties of the developed wheel steel with complex dispersion nitride and solid-solution hardening with silicon and manganese [24]. Compared to standard steel of K brand, steel of a conditional brand KAF has lower carbon content from 0.60–0.64 to 0.50–0.53 wt.%. In this case, dispersion nitride hardening provides:

- increase of the steel yield strength $\sigma_{0.2}$ up to 50 %;
- increase in impact toughness with +20 and –40 °C by 30–70 %;
- increase of fatigue endurance by 60–120 % and cyclic crack resistance by 30 %;
- 2.0–2.5 times increase in wear resistance under sliding and rolling friction.

Conclusion. Thus, the research on the effect of dispersion nitride hardening on the formation of the structure of high-carbon steels makes it possible to draw the following conclusions:

1. Nitrogen and vanadium alloying of high-carbon steels aimed at its additional effective dispersion nitride hardening provides the 2.5–3.0 times decrease in the size of austenitic grain during austenitization in the temperature range of 850–1000 °C due to the excess high-temperature dispersion nitride-vanadium phase which does not dissolve during austenitization.

2. Due to the dispersion of austenitic grains and the reduction of solid-solution nitrogen temperatures of $\gamma \rightarrow \alpha$ (P), $\gamma \rightarrow \alpha$ (B), $\gamma \rightarrow \alpha$ (M) transformations, the dispersion of perlite, bainite and martensitic structures occurs. In particular, the size of martensite needles decreases by 3–4 times, and the distance between cementite plates in perlite by 3.5–4.0 times.

3. The dispersion of the structure formed upon cooling after austenitization, as well as a decrease in the growth rate and coagulation of cementite particles, are the reasons for significant dispersion of pearlite, bainite and martensite tempering structures. This reduces the steel softening rate when increasing the tempering temperature. In comparison with standard steels tempered at 450 °C steels with dispersion nitride hardening have the same dispersion of cementite particles and hardness at tempering temperature increased by 150–200 °C. The size of coherent scattering blocks decreases by 1.5–2.0 times and microdistortion of the crystal lattice of ferritic phase steels decreases by 4 times. This predicts an increase in the ductility and toughness of the metal while maintaining its strength, which is confirmed by data on the mechanical and functional properties of the developed wheel steel with dispersion nitride hardening.

References

1. Tylkin M.A. *Spravochnik termista* [Handbook of a heat-treater]. Moscow, Metallurgiya Publ., 1981. 648 p.
2. Getmanova M.E., Grinshpon A.S., Sukhov A.V., Filippov G.A., Yandimirov A.A. Vliyanie neodnorodnosti struktury i nemetallicheskikh vklyucheniy na vyazkost razrusheniya kolesnoy stali [Influence of structure heterogeneity and nonmetallic inclusions upon destruction toughness of wheel steel]. *Stal* [Steel], 2007, no. 9, pp. 96–99.
3. Ostash O.P., Andreiko I.M., Kulyk V.V., Uzlov I.H., Babachenko O.I. Vtomnadovgovichnist staley zaliznichnikh kolis [Fatigue life of railway wheel steels]. *Fiziko-khimichna mekhanika materialiv* [Physicochemical mechanics of materials], 2007, no. 3, pp. 93–102.
4. Babaskin Yu.Z., Shipitsyn S.Ya., Kirchu I.F. *Konstruktsionnye i spetsialnye stali s nitridnoy fazoy* [Structural and special steels with nitride phase]. Kiev, Naukovaya dumka Publ., 2005. 371 p.
5. Lev I.E., Pokidyshev V.V., Lazarev B.G. *Analiz azotsoderzhashchikh soedineniy v splavakh zheleza* [Analysis of nitrogen-containing compounds in iron alloys]. Moscow, Metallurgiya Publ., 1997. 120 p.
6. Stepin V.V., Kurbatova V.I., Fedorova N.D., Stashkova N.V. *Opredelenie malykh kontsentratsiy komponentov v materialakh chernoy metallurgii. Spravochnik* [Determination of small concentrations of components in ferrous metallurgy materials. Handbook]. Moscow, Metallurgiya Publ., 1987. 256 p.
7. Shipitsyn S.Ya., Stepanova T.V., Zolotar N.Ya., Lev I.E., Isaeva L.E. Pererozpodil azotu ta vanadiyu pri austenizatsii stali z nitridnim zmitsnennem dlya zaliznichnikh kolis [Redistribution of nitrogen and vanadium in austenizating nitride strengthened steel for rail wheels]. *Metaloznavstvo ta obrobka metaliv* [Metal science and treatment of metals], 2014, no. 2, pp. 8–13.
8. Goldshteyn M.I., Gerasev M.A. *Rastvorenie karbidnykh i nitridnykh faz v stalyakh* [Dissolution of carbide and nitride phases in steels]. 1979. 120 p.
9. Goldshteyn M.I., Farber V.M. *Dispersionnoe uprochnenie stali* [Dispersion hardening of steel]. Moscow, Metallurgiya Publ., 1979. 208 p.
10. Kurdyumov G.V., Utevskiy L.M., Entin R.I. *Prevrashcheniya v zheleze i stali* [Transformations in iron and steel]. Moscow, Nauka Publ., 1977. 238 p.

11. Blanter M.E. *Teoriya termicheskoy obrabotki* [Theory of heat treatment]. Moscow, Metallurgiya Publ., 1972. 328 p.
12. Babaskin Yu.Z., Shipitsyn S.Ya., Aftandilyants E.G. *Ekonomnoe legirovanie stali* [Lean alloying of steels]. Kiev, Naukovaya dumka Publ., 1987. 184 p.
13. Haundros E.D. Grain boundary segregation. The current situation and future requirements. *Journal of Physics*, 1975, vol. 36, no. 10, pp. 117–134.
14. Utevskiy L.M. *Otpusknaya khrupkost* [Tempering embrittlement]. Moscow, Metallurgizdat Publ., 1961. 191 p.
15. Coats D.I., Henry A. The effect of dispersed nitrides on the oxidation of ferritic alloys. *Corrosion Science*, 1982, vol. 22, no. 10, pp. 973–989.
16. Wada M., Fukase S., Nishikawa O. Role of carbides in the grain boundary segregation of phosphorus in 2,25 Cr – 1 Mo steel. *Scripta Materialia*, 1982, vol. 16, no. 12, pp. 1373–1378.
17. Bokshteyn S.Z., Bokshteyn B.S. Struktura i diffuziya [Structure and diffusion]. *Metallovedenie i termicheskaya obrabotka stali* [Metallurgy and heat treatment of steel], 1983, vol. 2, pp. 63–65.
18. Gubenko S.I. Diffuzionnoe vzaimodeystvie nemetallicheskikh vklyucheniy i stalnoy matritsy pri nagreve i goryachey deformatsii [Diffusion interaction of nonmetallic inclusions and steel matrix during heating and hot deformation]. *Progressivnye metody termicheskogo uprochneniya v traktornom i selskokhozyaystvennom mashinostroenii* [Advanced methods of thermal hardening in tractor and agricultural machinery], 1983, pp. 82–87.
19. Franzoni U., Sturlese S., Goretzki H. Effetti della segregazione sulla cavizione intergranulare da scorrimento e sul comportamento a rottura nell acciaio 21/4 Cr – 1 Mo. *Bollettino tecnico Finsider*, 1983, no. 398, pp. 165–168.
20. Ibragimov Sh.Sh., Ilin A.M., Zashkvara V.V. Izuchenie segregatsii primesey vnedreniya na poverkhnosti razrusheniya stali 12Kh18N10T metodom elektronnoy Ozhe-spektroskopii [Study of the segregation of impurity embedding on the fracture surface of steel 12Kh18N10T by Auger electron spectroscopy]. *Poversknost: Fizika. Khimiya. Mekhanika* [Surface: Physics. Chemistry. Mechanics], 1984, no. 1, pp. 66–68.
21. Ekobori T. *Fizika i mekhanika razrusheniya i prochnosti tverdykh tel* [Physics and mechanics of fracture and strength of solids]. Moscow, Metallurgiya Publ., 1971. 264 p.
22. Sean M.H. Intergranular segregation phenomena studied by AES. *Journal de microscopie et de spectroscopie électroniques*, 1983, vol. 8, no. 3, pp. 177–181.
23. Suruki S., Obata M., Abiko K., Kimura H. Effect of Carbon on the Grain Boundary Segregation of Phosphorus in iron. *Scripta Materialia*, 1983, vol. 17, no. 11, pp. 1325–1328.
24. Shipitsyn S.Ya., Ostash O.P., Kulik V.V., Kirchu I.F., Novitskiy V.G. Novaya stal dlya zheleznodorozhnykh koles s povyshennym resursom [New steel for railway wheels with increased service life]. *Metall i lite Ukrainy* [Metal and casting in Ukraine], 2018, no. 5–6, pp. 52–59.

С.Я. ШИПИЦЫН, д-р техн. наук
заведующий лабораторией[1]
E-mail: odus@kiev.ptima.ua

В.И. ЖОРНИК, д-р техн. наук, доц.
начальник отделения технологий машиностроения и металлургии — заведующий лабораторией наноструктурных и сверхтвердых материалов[2]
E-mail: zhornik@inmash.basnet.by

Л.Е. ИСАЕВА, канд. хим. наук
доцент кафедры теории металлургических процессов и химии[3]
E-mail: isaevanmetau@gmail.com

П.Н. КУЧЕРЕНКО
младший научный сотрудник[1]
E-mail: odus@kiev.ptima.ua

Д.И. ЛИХОВЕЙ
младший научный сотрудник[1]
E-mail: odus@kiev.ptima.ua

[1]Физико-технологический институт металлов и сплавов НАН Украины, г. Киев, Украина
[2]Объединенный институт машиностроения НАН Беларуси, г. Минск, Республика Беларусь
[3]Национальная металлургическая академия Украины, г. Днепр, Украина

Поступила в редакцию 23.07.2019.

МЕТАЛЛОВЕДЧЕСКИЕ АСПЕКТЫ ВЛИЯНИЯ ДИСПЕРСИОННОГО НИТРИДНОГО УПРОЧНЕНИЯ НА СТРУКТУРУ ДОЭВТЕКТОИДНЫХ И ЭВТЕКТОИДНЫХ УГЛЕРОДИСТЫХ СТАЛЕЙ

Представлены результаты металловедческих исследований влияния микролегирования азотом и ванадием углеродистых сталей с содержанием углерода 0,5–0,8 масс.% на термодинамические и термокинетические параметры фазового перераспределения азота и ванадия, а также формирование феррито-перлитной, бейнитной и мартенситной структур и их трансформацию при высоком отпуске. Показано, что диспергирование сформировавшейся при охлаждении после аустенитизации структуры, а также уменьшение скорости роста и коагуляции цементитных частиц являются причиной суще-

ственного диспергирования структур отпуска перлита, бейнита и мартенсита. Отмечено положительное влияние диспергирования структур всех уровней на повышение механических свойств (предел текучести, ударная вязкость, износостойкость при трении скольжения и качения и др.) модифицированной микролегированием азотом и ванадием стали, что открывает хорошие перспективы эффективного применения сталей с дисперсионным нитридным упрочнением для производства железнодорожных колес и рельсов.

Ключевые слова: *углеродистые стали, легирование, дисперсионное нитридное упрочнение, феррито-перлитная, бейнитная и мартенситная структуры, аустенитизация, отпуск, фазовые превращения, железнодорожные колеса и рельсы*

Список литературы

1. Тылкин, М.А. Справочник термиста / М.А. Тылкин. — М.: Металлургия, 1981. — 648 с.
2. Влияние неоднородности структуры и неметаллических включений на вязкость разрушение колесной стали / М.Е. Гетманова [и др.] // Сталь. — 2007. — № 9. — С. 96–99.
3. Втомнадовговічність сталей залізничних коліс / О.П. Осташ [та ін.] // Фізико-хімічна механіка матеріалів. — 2007. — № 3. — С. 93–102.
4. Бабаскин, Ю.З. Конструкционные и специальные стали с нитридной фазой / Ю.З. Бабаскин, С.Я. Шипицын, И.Ф. Кирчу. — Киев: Наук. думка, 2005. — 371 с.
6. Лев, И.Е. Анализ азотсодержащих соединений в сплавах железа / И.Е. Лев, В.В. Покидышев, Б.Г. Лазарев. — М.: Металлургия, 1997. — 120 с.
6. Определение малых концентраций компонентов в материалах черной металлургии: справочник / В.В. Степин [и др.]. — М.: Металлургия, 1987. — 256 с.
7. Перерозподіл азоту та ванадію при аустенізації сталі з нітридним зміцненням для залізничних коліс / С.Я. Шипицин [та інш.] // Металознавство та обробкаметалів. — 2014. — № 2. — С. 8–13.
8. Гольдштейн, М.И. Растворение карбидных и нитридных фаз в сталях / М.И. Гольдштейн, М.А. Герасьев // Изв. вузов. Металлы. — 1979. — 120 с.
9. Гольдштейн, М.И. Дисперсионное упрочнение стали / М.И. Гольдштейн, В.М. Фарбер. — М.: Металлургия, 1979. — 208 с.
10. Курдюмов, Г.В. Превращения в железе и стали / Г.В. Курдюмов, Л.М. Утевский, Р.И. Энтин. — М: Наука, 1977. — 238 с.
11. Блантер, М.Е. Теория термической обработки / М.Е. Блантер. — М.: Металлургия, 1972. — 328 с.
12. Бабаскин, Ю.З. Экономное легирование стали / Ю.З. Бабаскин, С.Я. Шипицын, Е.Г. Афтандилянц. — Киев: Наук. думка, 1987. — 184 с.
13. Haundros, E.D. Grain boundary segregation. The current situation and future requirements / E.D. Haundros // J. Phys. — 1975. — Vol. 36, No. 10. — Pp. 117–134.
14. Утевский, Л.М. Отпускная хрупкость / Л.М. Утевский. — М.: Металлургиздат, 1961. — 191 с.
15. Coats, D.I. The effect of dispersed nitrides on the oxidation of ferritic alloys / D.I. Coats, A. Henry // Corros. Sci. — 1982. — Vol. 22, No. 10. — Pp. 973–989.
16. Wada, M. Role of carbides in the grain boundary segregation of phosphorus in 2,25 Cr – 1 Mo steel / M. Wada, S. Fukase, O. Nishikawa // Scr. met. — 1982. — Vol. 16, No. 12. — Pp. 1373–1378.
17. Бокштейн, С.З. Структура и диффузия // Металловедение и термическая обработка стали: справ. / С.З. Бокштейн, Б.С. Бокштейн; под ред. М.Л. Берштейна, А.Г. Рахштадта. — М.: Металлургия, 1983. — № 2. — С. 63–65.
18. Губенко, С.И. Диффузионное взаимодействие неметаллических включений и стальной матрицы при нагреве и горячей деформации / С.И. Губенко // Прогрессивные методы термического упрочнения в тракторном и сельскохозяйственном машиностроении. — Ростов-на-Дону, 1983. — С. 82–87.
19. Franzoni, U. Effetti della segregazione sulla cavizione intergranulare da scorrimento e sul comportamento a rottura nell acciaio 21/4 Cr – 1 Mo / U. Franzoni, S. Sturlese, H. Goretzki // Boll. tech. Finsid. — 1983. — No. 398. — Pp. 165–168.
20. Ибрагимов, Ш.Ш. Изучение сегрегации примесей внедрения на поверхности разрушения стали 12Х18Н10Т методом электронной Оже-спектроскопии / Ш.Ш. Ибрагимов, А.М. Ильин, В.В. Зашквара // Поверхность: Физика. Химия. Механика. — 1984. — № 1. — С. 66–68.
21. Екобори, Т. Физика и механика разрушения и прочности твердых тел / Т. Екобори. — М.: Металлургия, 1971. — 264 с.
22. Sean, M.H. Intergranular segregation phenomena studied by AES / M.H. Sean // J. Microsc. Et Spectrosc. Electron. — 1983. — Vol. 8, No. 3. — Pp. 177–181.
23. Effect of Carbon on the Grain Boundary Segregation of Phosphorus in iron / S. Suruki [et al.] // Scr. met. — 1983. — Vol. 17, No. 11. — Pp. 1325–1328.
24. Новая сталь для железнодорожных колес с повышенным ресурсом / С.Я. Шипицын [и др.] // Металл и литье Украины. — 2018. — № 5–6. — С. 52–59.